Phys. Status Solidi C **8**, No. 4, 1204–1207 (2011) / **DOI** 10.1002/pssc.201000838

physica status solidi pss c
www.pss-c.com
current topics in solid state physics

Intrasubband transitions in cubic AlN/GaN superlattices for detectors from near to far infrared

Christian Mietze*[,1], E. A. DeCuir, Jr.[2], M. O. Manasreh[2], K. Lischka[1], and D. J. As[1]

[1] University of Paderborn, Department of Physics, Warburger Str. 100, 33098 Paderborn, Germany
[2] Department of Electrical Engineering, University of Arkansas, 3217 Bell Engineering Center, Fayetteville, Arkansas 72701, USA

Received 13 August 2010, revised 14 September 2010, accepted 14 September 2010
Published online 1 February 2011

Keywords cubic, AlN, GaN, MBE, inter- and intrasubband transitions

* Corresponding autor: e-mail cmietze@mail.upb.de

We report the growth of cubic GaN/AlN superlattices by plasma-assisted molecular beam epitaxy on 3C-SiC substrates. The samples consist of 100 nm thick unintentionally doped GaN buffer and 20-40 period superlattices of silicon doped GaN quantum wells embedded in undoped AlN barriers. The thickness of the AlN barriers is varied between 1.5 nm-3.2 nm, while the thickness of the GaN well varies between 1.5 nm-12.5 nm. The growth was controlled by in situ reflection high energy electron diffraction. The structural properties of our samples were studied by high resolution x-ray diffraction. Two superlattice satellite peaks in the x-ray spectra reveal a high structural perfection of the active region. Clear evidence for inter- and intrasubband transitions was observed in photoluminescence, absorbance and photoconductivity spectra measured at room temperature. Model calculations show the possibility to fabricate devices for the near- and far infrared region.

© 2011 WILEY-VCH Verlag GmbH & Co. KGaA, Weinheim

1 Introduction

Intrasubband transitions in superlattices (SL) form the basis for optoelectronic devices like quantum well infrared photodetectors and quantum cascade lasers [1]. Due to the large band gap difference between AlN and GaN this group of III-nitrides offers intrasubband transitions tunable over a wide spectral range. In hexagonal GaN and AlN strong intrinsic piezoelectric and pyroelectric fields are present at the hetero-interfaces. These built in fields are undesirable for optical devices, which for example use intersubband transitions in thick SL structures. Growth of the metastable cubic phase of GaN and AlN is a possibility to avoid these built in fields, because of the cubic crystal symmetry. This makes the cubic system a very promising candidate for device fabrication. It has already been shown by infrared absorbance measurements that the technologically important 1.5 µm infrared region can be reached using cubic GaN/AlN superlattices [2, 3].

2 Experimental

All samples containing quantum structures were grown by plasma assisted molecular beam epitaxy (MBE) at $T_{substrate}$=720 °C on 10 µm thick 3C-SiC on top of Si. A 100 nm thick cubic GaN (c-GaN) buffer layer was deposited on the 3C-SiC substrate. The c-GaN layers were grown under a 1 ML Ga coverage while the thickness of the c-AlN layers was controlled by reflection high energy electron diffraction (RHEED) oscillations. Further details about growth of c-GaN are given in [4]. For our first series of GaN/AlN samples (series A) superlattices with 20 periods were grown. The thickness of the AlN barriers was 1.5 nm and the well width of the GaN quantum wells was varied between 1.6 nm and 2.7 nm. The SL was followed by another 100 nm thick c-GaN cap layer. During deposition of the SL, growth was interrupted for 20 s after each layer. This procedure allowed excess metal to evaporate from the surface. For the second series of samples (series B) the thickness of the c-GaN cap layer was reduced to 10 nm to minimize absorption in the cap layer for PL measurements. The number of SL periods was increased to 40 to increase the absorption in the active layer. The thickness of the c-AlN barriers was 3.2 nm and the thickness of the c-GaN wells in series B was varied between 2 nm and 12.5 nm. Structural properties of our samples were characterized by high resolution x-ray diffraction (HRXRD). From the diffraction profiles lattice parameter and the relaxation of the superlattice samples were measured.

© 2011 WILEY-VCH Verlag GmbH & Co. KGaA, Weinheim

Bound state energy levels are calculated using a Poisson-Schrödinger solver (1D Poisson) [5]. Energy differences between the bound states are calculated for different well and barrier widths. These calculated values for intra- and intersubband transitions are compared to the experimental data of PL and infrared absorption measurements.

3 Results and discussion

3.1 High resolution X-ray diffraction From asymmetrical reciprocal space maps of the (113) reflex of the superlattices grown on c-GaN one can investigate the relaxation of the superlattices. The lattice period of the superlattice samples is determined from ω–2θ scans using a high resolution x-ray diffractometer. In Ref. [3] we showed that samples with the structure of series A are pseudomorphically strained to the buffer layer. Fig. 1 shows an asymmetrical reciprocal space map of the (113) reflex of a sample of series B. The positions of the superlattice satellites reveal that the superlattice has a lattice parameter slightly different from that of the buffer layer. This can be explained by the thicker AlN barriers. Due to the comparable volume fraction of c-GaN and c-AlN a lattice parameter between c-GaN and c-AlN is formed within the superlattice resulting in a strain distribution. Another difference between series A and B: series B has a thinner cap layer which does not strain the SL from the top side. From the positions of superlattice satellites in ω–2θ scans of the (002) reflex the lattice parameter of the superlattice was calculated. Furthermore the thicknesses of the single layers were estimated from HRXRD simulations using dynamical scattering theory [6]. The obtained layer thicknesses are in good agreement with those measured by RHEED.

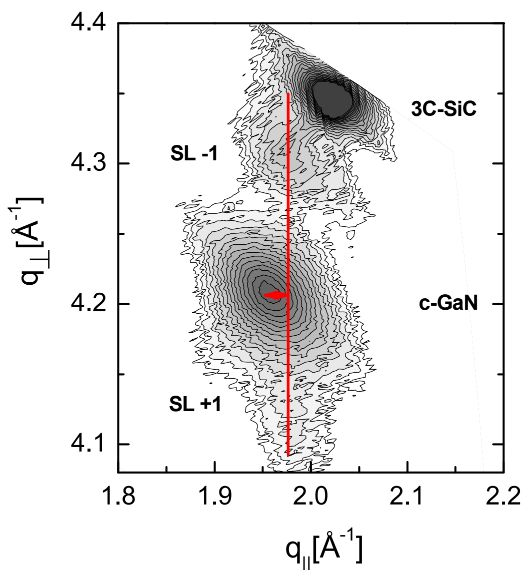

Figure 1 RSM of the (113) reflex for a sample of series B.

3.2 Infrared absorbance/photoconductivity Figure 2 shows the infrared absorbance spectrum and the photoconductivity spectrum of a series A sample with 1.6 nm thick GaN wells and 1.5 nm AlN barriers. We observe clear absorption in the infrared region. We find the same peak wavelength for absorbance and photoconductivity. From the symmetric shape of the absorption and photocunductivity band we conclude, that the observed transition is a transition between two separated minibands since a transition from a miniband to the continuum state would cause a stronger asymmetry of the spectrum. In the following we define the absorbance peak energy in the spectra as the intrasubband transition energy. We observe absorbance with peak energies between 800 meV and 600 meV (1.5 μm-2.1 μm).

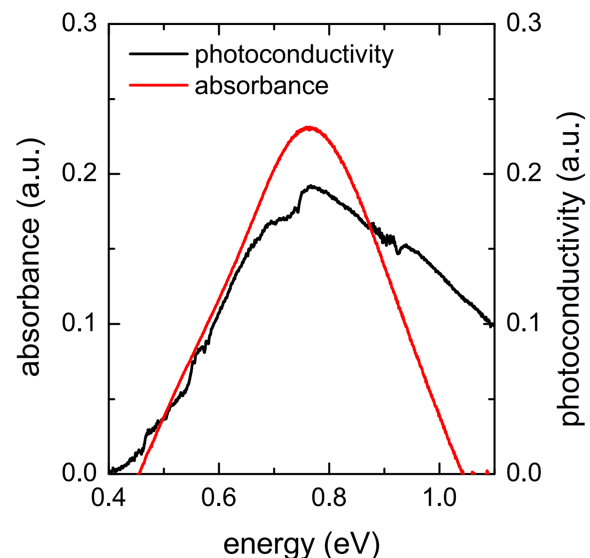

Figure 2 Room temperature absorbance and photoconductivity (T=77 K) spectra of a sample of series A with 1.6 nm GaN QWs.

3.3 Photoluminescence spectroscopy The room temperature photoluminescence spectra for series A and B are plotted in Fig. 3 and Fig 4. Clear luminescence corresponding to intersubband transitions in the superlattice is observed. In addition a clear red shift of the emission energy with increasing well width is measured. The fact that luminescence of the superlattice can be observed proves the high structural quality of the samples and the presence of subbands. The larger linewidths for thinner QWs can be explained by the increased influence of roughness and thickness fluctuations on the transition energy for thin QWs. The luminescence of series B shows minor noise and no luminescence of bulk GaN due to the thinner cap layer and the increased number of periods. For this series of samples the transition energy shift saturates for well widths exceeding 11 nm. As excitation source a HeCd laser emitting at 325 nm was used.

 © 2011 WILEY-VCH Verlag GmbH & Co. KGaA, Weinheim

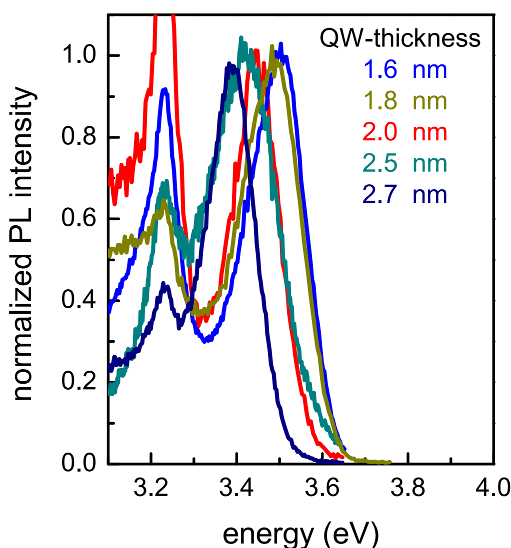

Figure 3 Room temperature PL spectra of sample series A.

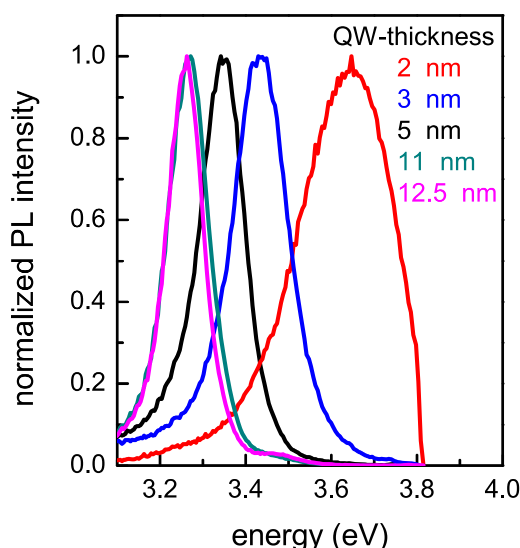

Figure 4 Room temperature PL spectra of sample series B.

The transition energy of the superlattice photoluminescence is compared to calculated values for intersubband transitions using a one dimensional Poisson-Schrödinger solver. For the transition energy calculations a conduction band to valence band offset ratio of 60:40 was assumed. Strain induced modification of the band gap energy was also taken into account using the deformation potentials given in Table 1.

Table 1 Parameters used for transition energy calculations [7-12].

Parameter	c-AlN	c-GaN
E_G	5.9 eV	3.2 eV
m^*_{hh}/m_0	1.2	0.8
m^*_{lh}/m_0	0.33	0.18
m_e/m_0	0.19	0.15
a_C	-2.77 eV	-6.8 eV
c_{11}	296 GPa	304 GPa
c_{12}	156 GPa	152 GPa
$\Delta E_C:\Delta E_V$	60:40	

Figure 5 shows calculated and experimental data for intersubband transitions. Experimental and calculated values show only small deviations over a wide spectral range.

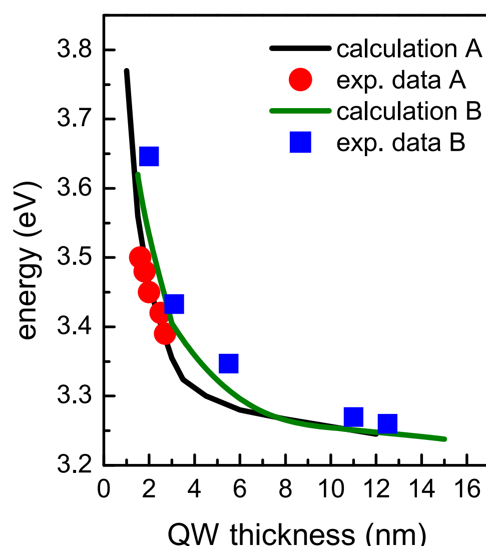

Figure 5 Calculated intersubband transition energies for series A (black curve) and B (green curve) and experimental data from photoluminescence spectroscopy for series A (red dots) and B (blue squares).

The calculated electronic intrasubband transition energies for both series of samples are plotted in Fig. 6 versus QW width. The calculated values for series A are represented by the black line and the measured values by red dots. We find good agreement between calculated and measured transition energies. The deviations between experimental and calculated data can be explained by thickness fluctuations in the superlattice. The agreement between calculation and experiment from two independent measurement methods shows that our calculations describe this system very well.

The green dash-dotted line shows a calculation assuming the structure of series B samples however no experimental data are available for this series yet.

© 2011 WILEY-VCH Verlag GmbH & Co. KGaA, Weinheim

The calculated data shown in Fig. 6 demonstrate that intrasubband transitions in cubic III-nitride superlattices can cover the spectral range from infrared 800 meV (1.5 μm) down to the terahertz region 28 meV (45 μm). Far infrared absorption measurements with our samples are currently under way.

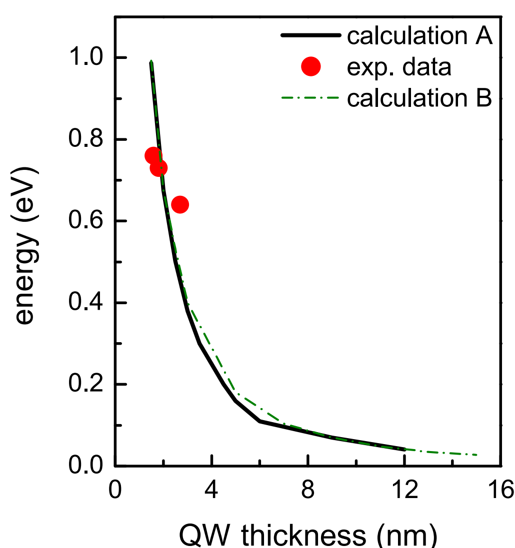

Figure 6 Calculated intrasubband band transition energies for series A and B (black and green dotted line) and experimental data from absorbance spectroscopy for series A (red dots).

4 Conclusions

Nonpolar zincblende GaN/AlN superlattices with intersubband transitions in the range of 3.2 eV-3.7 eV and intrasubband transitions in the spectral range of 0.6 eV-0.8 eV were fabricated by plasma assisted molecular beam epitaxy. The thicknesses of the single layers were observed in-situ by RHEED and confirmed by HRXRD measurements and simulations. Inter- and intrasubband transitions were observed at T=300 K. We find a red shift with increasing well width in PL and absorption/photoconductivity measurements due to smaller confinement energies. The experimental results are compared to calculated values using a one dimensional Poisson-Schrödinger solver showing good agreement. Our experiments together with the model calculation show that superlattice structures based on cubic III-nitrides can form the basis for devices operating in the near and far infrared region.

Acknowledgements The work at Paderborn was supported by German Science Foundation (DFG, project As (107/4-1)). The work at University of Arkansas was funded by the Air Force Office of Scientific Research and by the Arkansas Science & Technology Authority.

References

[1] G. Gmachl and H.M. Ng, Electron. Lett. **39**, 567 (2003).
[2] E.A. DeCuir, E. Fred, M.O. Manasreh, J. Schörmann, D.J. As, and K. Lischka, Appl. Phys. Lett. **91**, 041911 (2007).
[3] C. Mietze, E.A. DeCuir, M.O. Manasreh, K. Lischka, and D.J. As, Phys. Status Solidi C **7**(1), 64 (2010).
[4] J. Schörmann, S. Potthast, D.J. As, and K. Lischka, Appl. Phys. Lett. **90**, 041918 (2007).
[5] I. H. Tan, G. Snider, and E. L. Hu, J. Appl. Phys. **68**, 4071 (1990).
[6] O. Brandt, P. Waltereit, and K.H. Ploog, J. Phys. D: Appl. Phys. **35,** 577 (2002).
[7] Y. Suzuki, M. Shinbara, H. Kii, and Y. Chikaura, J. Appl. Phys. **101**, 063516 (2007).
[8] S. Pugh, D.J. Dugdale, S. Brand, and R.A. Abram, Semicond. Sci. Technol. **14**, 23 (1999).
[9] C.G. van de Walle and J. Neugebauer, Appl. Phys. Lett. **70**(19), 2577 (1997).
[10] K. Kim, W.R.L. Lambrecht, and B. Segall, Phys. Rev. B **53**, 16310 (1996).
[11] I. Petrov, E. Mojab, R.C. Powell, and J.E. Greene, Appl. Phys. Lett. **60**, 2491 (1992).
[12] M. Röppischer, R. Goldhahn, G. Rossbach, P. Schley, C. Cobet, N. Esser, T. Schupp, K. Lischka, and D.J. As, J. Appl. Phys. **106**(7), 076104 (2009).

© 2011 WILEY-VCH Verlag GmbH & Co. KGaA, Weinheim